



Silica sputtering as a novel collective stationary phase deposition for microelectromechanical system gas chromatography column: Feasibility and first separations

J. Vial^{a,*}, D. Thiébaud^a, F. Marty^b, P. Guibal^c, R. Haudebourg^c, K. Nacheff^c, K. Danaie^c, B. Bourlon^c

^a Laboratoire Sciences Analytiques, Bioanalytiques et Miniaturisation, ESPCI Paristech – CNRS UMR PECSA 7195, 10 rue Vauquelin, 75005 Paris, France

^b ESIEE Paris, 2 boulevard Blaise Pascal, 93162 Noisy le Grand, France

^c Schlumberger, MEMS Technology Center, 10b rue Blaise Pascal, 78990 Elancourt, France

ARTICLE INFO

Article history:

Available online 21 December 2010

Keywords:

MEMS technology
Gas chromatography
Stationary phase
Sputtering
Miniaturization

ABSTRACT

Since the late 1970s, approaches have been proposed to replace conventional gas chromatography apparatus with silicon-based microfabricated separation systems. Performances are expected to be improved with miniaturization owing to the reduction of diffusion distances and better thermal management. However, one of the main challenges consists in the collective and reproducible fabrication of efficient microelectromechanical system (MEMS) gas chromatography (GC) columns. Indeed, usual coating processes or classical packing with particulate matters are not compatible with the requirements of collective MEMS production in clean room facilities. A new strategy based on the rerouting of conventional microfabrication techniques and widely used in electronics for metals and dielectrics deposition is presented. The originality lies in the sputtering techniques employed for the deposition of the stationary phase. The potential of these novel sputtered stationary phases is demonstrated with silica sputtering applied to the separation of light hydrocarbons and natural gases. If kinetic characteristics of the sputtered open tubular columns were acceptable with 2500 theoretical plates per meter, the limited retention and resolution of light hydrocarbons led us to consider semipacked sputtered columns with rectangular pillars allowing also significant reduction of typical diffusion distances. In that case separations were greatly improved because retention increased and efficiency was close to 5000 theoretical plates per meter.

© 2010 Elsevier B.V. All rights reserved.

1. Introduction

Chromatography is a first choice laboratory technique for the analysis and quantification of complex mixtures of gas or liquid volatile components. While laboratory instruments have been used for more than 50 years, intense efforts are done today in research institutes and companies R&D departments to replace laboratory instruments by “lab-on-a-chip” sensors [1] that are less versatile but more adapted to a specific dedicated task. Miniaturization of chromatographic systems presents many advantages. Effectively, according to the chromatographic theory, the reduction of the typical dimensions of the systems favours the kinetics of the exchanges by decreasing the lengths on which the solutes must diffuse during mass transfers between mobile and stationary phases [2,3]. Moreover, the lower thermal capacity of the technological bricks (column, injector, detector, . . .) opens the way

to faster thermal management, with lower power consumption [4].

Since the late 1970s, technology from the microelectronics industry has been used to build gas chromatography (GC) columns, leading to the realisation of various prototypes [5–7]. Despite the growing number of publications showing the potential of microfabricated columns, and as underlined recently by Tienpont et al. [7], highly miniaturized systems based on microelectromechanical systems (MEMS) are not yet available for routine analysis. While it is rather easy to make channels of dimensions compatible with GC requirements into a silicon or glass chip, putting a stationary phase inside the channel is everything but trivial. Indeed, usual coating processes or classical packing with particulate matters are not compatible with extreme miniaturization and the requirements of production in clean room facilities. Thus, the coating of the walls from a solution of polydimethylsiloxane diluted in an appropriate solvent requires an additional fabrication step that must be carried out “offline” from the microfabrication process. Consequently, for GC MEMS columns, one of the main challenges consists

* Corresponding author. Tel.: +33 1 40 79 47 79; fax: +33 1 40 79 47 76.
E-mail address: Jerome.vial@espci.fr (J. Vial).

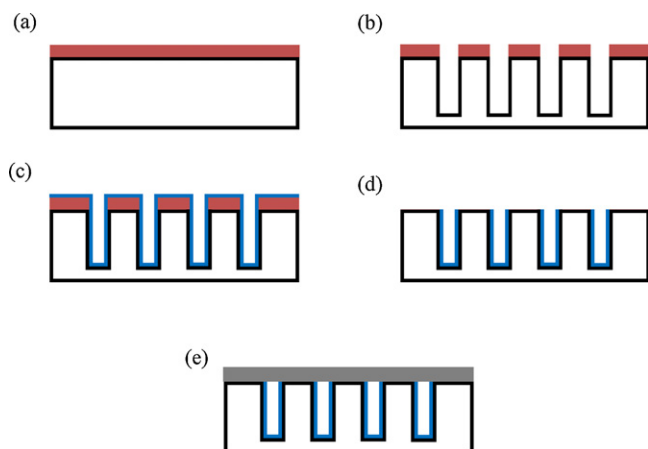


Fig. 1. Main fabrication steps of the silica-coated microchannels: (a) deposition of photoresist by spincoating, (b) photolithography and etching by DRIE, (c) sputtering of silica, (d) lift-off, and (e) silicon-pyrex anodic bonding.

in finding a collective and reproducible fabrication process to incorporate a stationary phase inside the channel [8–11]. To address this issue, a new original strategy was applied. It was based on the rerouting of a conventional microfabrication technique widely used in electronics for metals and dielectrics deposition: sputtering.

In this paper, the potential of these novel stationary phases will be evaluated with the application of silica sputtering to the separation of light hydrocarbons and natural gases [12,13]. Kinetic characteristics of MEMS sputtered open tubular columns with coatings of different thicknesses will be compared. While a thicker stationary phase generally helps to increase retention and sample capacity, the drawback is the loss of separation efficiency. To overcome this limitation, semipacked columns with high-aspect-ratio pillars [14–16] also subjected to silica sputtering will be evaluated from a kinetic point of view.

2. Experimental

2.1. MEMS column fabrication

Columns have been fabricated on a 400- μm -thick double-sided polished silicon wafer. As illustrated in Fig. 1, a 3- μm -thick layer of SIPR-3251M-3.0 was deposited on the top side of the wafer and patterned with the columns mask. Channels were etched to a depth of 100 or 125 μm by deep reactive-ion etching (DRIE) using an anisotropic standard Bosch process. Typical width of the columns fabricated varied from 50 μm to 200 μm . This process is based on the use of the alternative steps involving SF_6 and C_4F_8 . SF_6 etches the silicon and C_4F_8 passivates the surface. A thin film of silica is then deposited onto the microchannels. To that end, sputtering, a classical technique used in MEMS technology, has been used. The general principle of sputtering can be described in three main steps. First, a gas is ionized inside a vacuum chamber between the substrate and a target made of the material to be deposited. Then, generated ions are accelerated towards the target. Collisions of the ions with the target induce ejections or sputtering of target atoms finally deposited onto the substrate. The purity of the silica target used for fabrication is 99.995%. A scheme of sputtering process is presented in Fig. 2. After lift-off of the resist in acetone, the substrate was cleaned in a mixture of H_2O_2 and H_2SO_4 solution. The silicon wafer was anodically bonded to a 250- μm -thick Pyrex substrate. In the similar manner, inlet and outlet back access holes were etched on the back side of the wafer to a depth of 330 μm . After fabrication, the wafer was diced to obtain ~ 1.5 -cm squared MEMS columns. Two ~ 5 -cm-long 100- μm ID fused silica capillaries were plugged and glued on the inlet and outlet vertical holes on the back of the MEMS column silicon chip (Fig. 3). In the case of semipacked columns with pillars, typical diffusion distances are no longer the column width but rather the pillar to pillar distance, i.e. 10 μm . The stationary phase film thickness was determined using scanning electron microscope imaging of a cross sectional view of the column. The sputtered silica can be easily distinguished from the

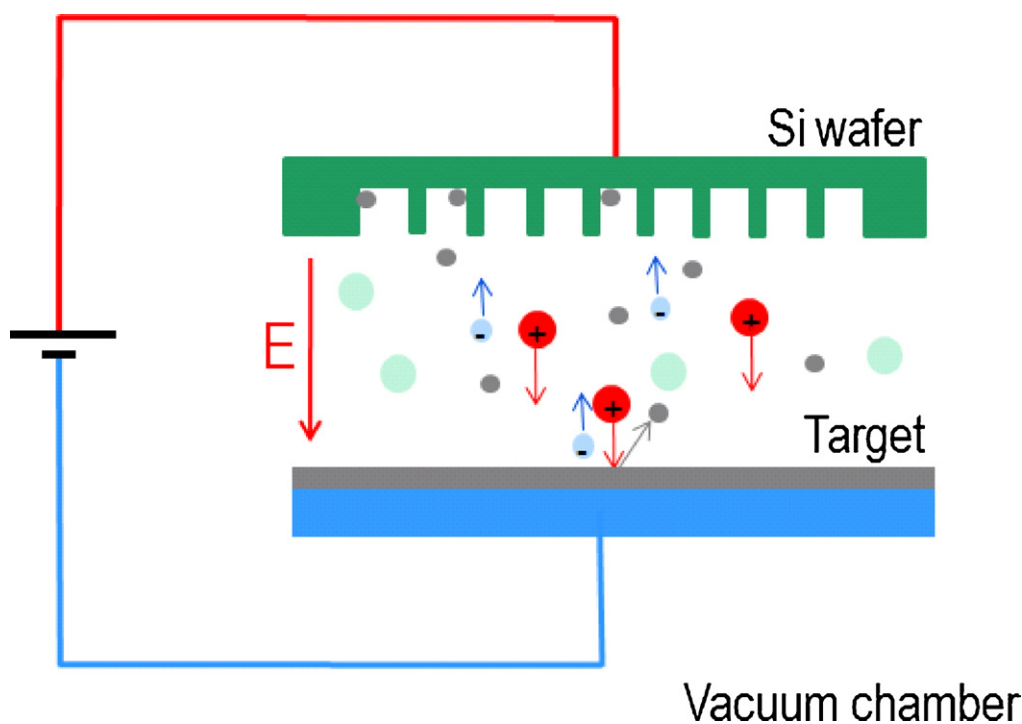


Fig. 2. Scheme of the sputtering process. Collisions of the ions of the ionized gas with the target induce ejection of target atoms which are then deposited on the surface of the silicon wafer.

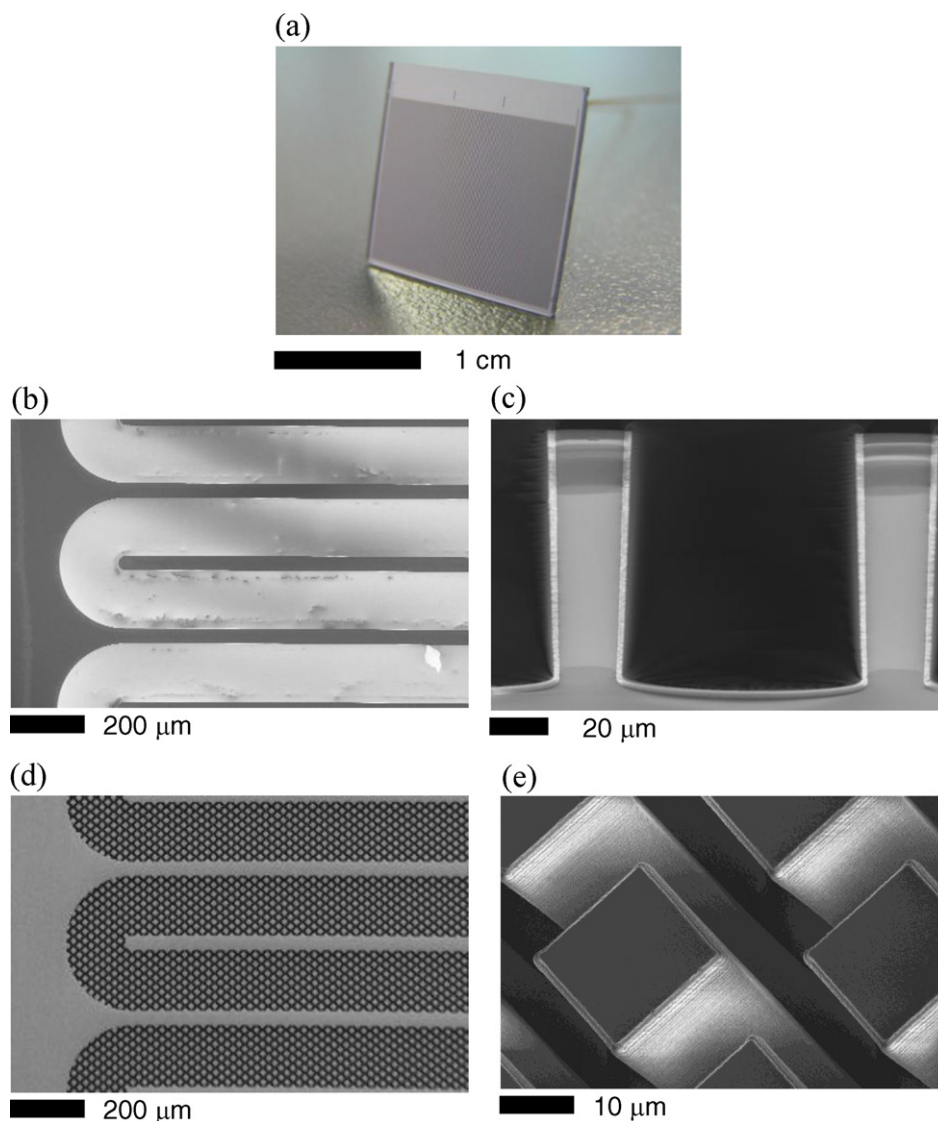


Fig. 3. (a) Picture of a MEMS column after fabrication. Capillaries are glued to the holes on the back of the silicon chip, connecting inlet and outlet of the microchannel. (b) SEM image of an open microchannel coated with silica. (c) Cross-sectional view of a silica-coated microchannel. The $\sim 3 \mu\text{m}$ silica coating appears in white color. (d) SEM image of a microchannel with particle-like micropillars. (e) Zoom view of the micropillars coated with a silica film.

support and a resolution of the order of 10 nm can be achieved. The uniformity along the axis of the column is better than 5%. When the depth to width aspect ratio is close to 1, differences in film thickness between the top and bottom of the walls of the column are limited to around 25%.

2.2. Analytical GC device used for columns evaluation

A conventional GC was used to evaluate the MEMS columns. As the aim of our study was to provide a first evaluation of this novel sputtered stationary phase, no specific modifications were brought to the GC to reduce extra column band broadening as it is described in the literature [17,18]. Experiments were carried out on a Varian 3800. The chromatograph was equipped with a 1079 split-splitless injector and a flame ionization detection (FID) system. The injector temperature was set at 200°C . It worked in split mode with a split ratio adjusted to transfer the smallest amount of analyte into the column, allowing efficiency determinations. Detector temperature was set at 300°C , makeup gas flow rate at 30 mL min^{-1} , hydrogen flow rate at 30 mL min^{-1} , and air flow rate at 300 mL min^{-1} . Helium was used as carrier gas at typically 0.3 mL min^{-1} . Unless

there were other indications, the oven was shut down and experiments were carried out at ambient temperature. The MEMS column was then connected to the injector and detector by means of two $\sim 15\text{-cm}$ -long $100\text{-}\mu\text{m}$ fused silica tubing with PressFit connectors (BGB Analytik).

2.3. Gases

Helium was purchased from Air Liquide (grade Alphagaz 1). Hydrogen was obtained from a F-DBS NMH2 250 hydrogen generator. A compressor with F-DBS GC 1500 air generator and Donaldson filters were used for the air gas source.

2.4. Gas samples

Gas samples were prepared by filling a sampling bag with methane, ethane, propane and butane, obtained from the corresponding gas cylinders (Praxair). A 0- to $5\text{-}\mu\text{L}$ or 0- to $10\text{-}\mu\text{L}$ glass syringe was used to sample the gas mixture and inject it into the GC injector.

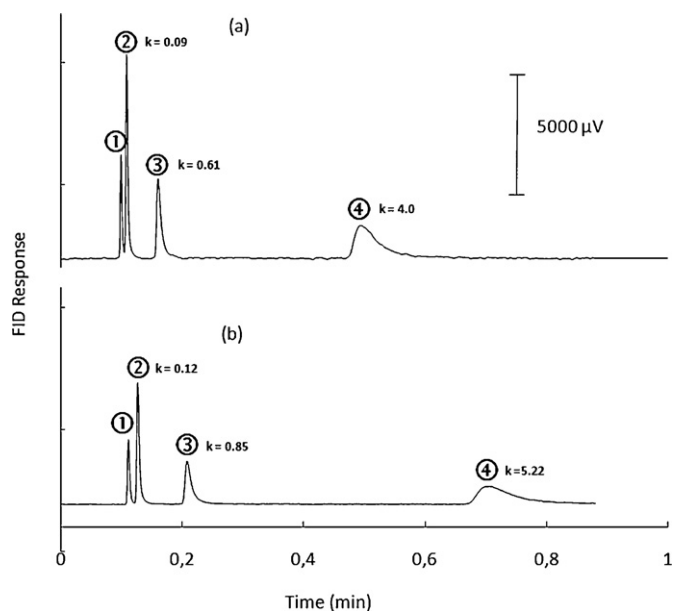


Fig. 4. Separation of light hydrocarbons: methane ①, ethane ②, propane ③, butane ④. MEMS column ($75 \mu\text{m} \times 100 \mu\text{m} \times 220 \text{cm}$), sputtered silica, injected volume of $2 \mu\text{L}$, split ratio of 200. MEMS column inside the GC oven: (a) coating thickness $\sim 0.75 \mu\text{m}$; He, 20 psi; 30°C ; linear velocity, 42 cm/s ; (b) coating thickness $\sim 1.5 \mu\text{m}$; He, 15 psi; 30°C ; linear velocity 37 cm/s .

2.5. Data acquisition

A commercial acquisition card was used to interface the Varian GC with a computer. Galaxie 1.9 was used as acquisition software. For the Van Deemter plots, efficiency (N) was calculated from the width at half height (δ) by the formula $N = 5.54(t_r/\delta)^2$. Linear velocity of the gas was obtained from the methane peak, supposed not retained. Measures were repeated three to five times and the values of the theoretical plate numbers were averaged.

3. Results and discussion

Results obtained with open tubular and semi-packed silica sputtered columns, at different sputtering durations, are presented.

3.1. Open tubular columns

Open tubular columns, obtained with three different sputtering durations, were evaluated. Fig. 4 gives the chromatograms of light hydrocarbons obtained in optimal carrier gas velocity conditions for sputtering coatings thickness of $0.75 \mu\text{m}$ and $1.5 \mu\text{m}$. Retention mechanism on silica gel used in classical solid phase GC [12,13] involved adsorption on the active sites [19]. Similar mechanism are expected for the sputtered silica stationary phase.

As expected, the retention increased with the thickness of the coating [20]. If the methane is considered as not retained and is used as a void volume marker, the increase in retention factors between coatings thickness of $0.75 \mu\text{m}$ and $1.5 \mu\text{m}$ averages 34%. For a coating of $1.5 \mu\text{m}$, this increase in retention enabled achievement of a baseline resolution for methane and ethane while they were slightly coeluted for a coating thickness of $0.75 \mu\text{m}$. These results confirmed that increasing coating duration, which governs the coating thickness, is a primary mean to increase retention of light hydrocarbons. It also confirms that sputtered silica is a porous solid allowing diffusion of hydrocarbons; otherwise film thickness would have no effect on retention. Nevertheless, thick coatings could present the same drawbacks as thick films and could lead to a decrease in efficiency resulting from the negative contribution

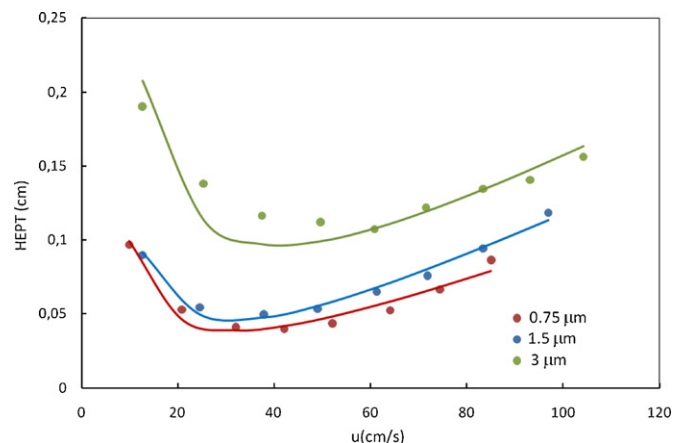


Fig. 5. Kinetic evaluation for silica-sputtered MEMS column ($75 \mu\text{m} \times 100 \mu\text{m} \times 220 \text{cm}$) obtained for three different thicknesses of silica film coating (about $0.75 \mu\text{m}$, $1.5 \mu\text{m}$, $3 \mu\text{m}$). Solute: ethane, injected volume of $2 \mu\text{L}$, split ratio of 200. Carrier: He. Temperature: ambient temperature.

of thick films to the mass transfer process. To answer this matter a kinetic evaluation was carried out on three similar MEMS columns that had undergone three different coating durations. The Van Deemter curves obtained are given in Fig. 5.

As expected, the thicker the film, the lower the efficiency. Therefore, if efficiency could reach 2500 theoretical plates per meter for a $0.75 \mu\text{m}$ coating thickness, it was only 900 theoretical plates per meter for a coating thickness of $3 \mu\text{m}$. Curve fitting with the Van Deemter equation ($H = A + (B/u) + Cu$) was performed by means of the solver of Excel. Given the difficulty of making experimental measurements, these first investigations did not allow conclusions about significant trends, either about the evolution of the C term as a function of coating thickness or about the value of the optimal velocity. Nevertheless, there appeared to be a small increase of the curve slopes at high velocities when the coating thickness increased from $0.75 \mu\text{m}$ to $1.5 \mu\text{m}$. Using the column depth as normalization factor, reduced plate height are in the 5–10 range. Such values confirmed the presence of extra band broadening coming from the classical GC used for this first evaluation and limits the possible kinetic interpretations at this stage of this new GC chip development.

MEMS technologies are known to be a first choice technology for production at a large scale of reproducible components. The repeatability of the whole fabrication process, including etching of the channels and silica sputtering, was confirmed by comparing

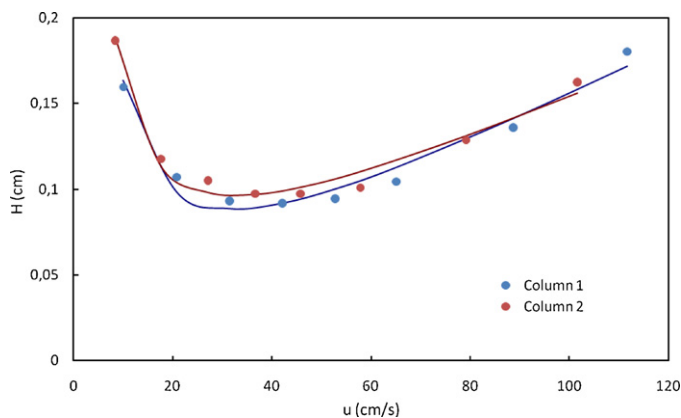


Fig. 6. Kinetic comparison of two silica-sputtered MEMS columns ($100 \mu\text{m} \times 100 \mu\text{m} \times 220 \text{cm}$) coated with a $3 \mu\text{m}$ -thick silica film. Solute: ethane, injected volume of $1 \mu\text{L}$, split ratio of 200. Carrier: He. Temperature: 30°C .

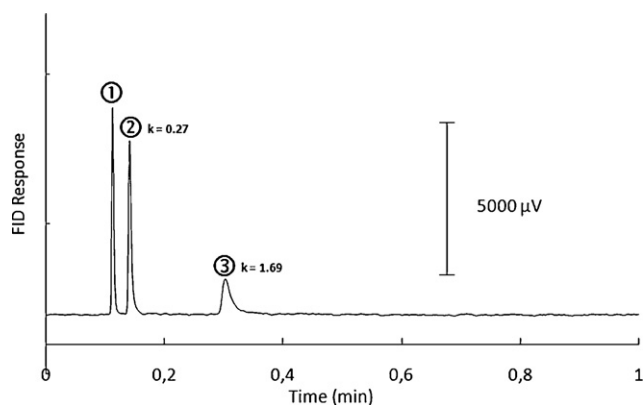


Fig. 7. Separation of light hydrocarbons: methane ①, ethane ②, propane ③. Semi-packed MEMS column ($225\ \mu\text{m} \times 125\ \mu\text{m} \times 110\ \text{cm}$) with pillars ($17\ \mu\text{m} \times 17\ \mu\text{m} \times 125\ \mu\text{m}$), sputtered silica, injected volume of $2\ \mu\text{L}$, split ratio of 5. MEMS column inside the GC oven; coating thickness $\sim 1.5\ \mu\text{m}$; He 100 psi; 30°C ; linear velocity of $21\ \text{cm/s}$.

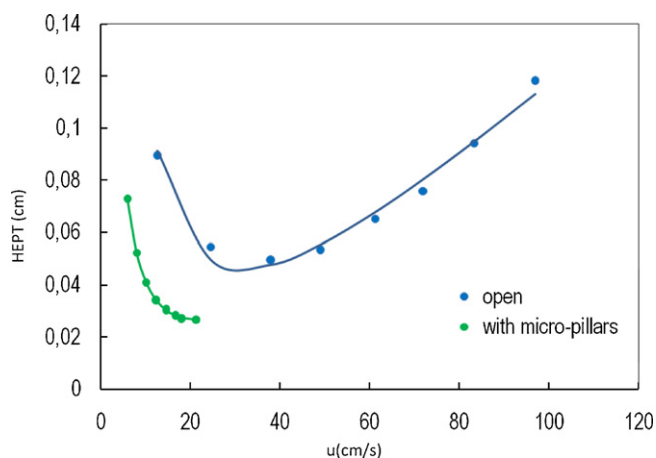


Fig. 8. Kinetic comparison of open and semipacked silica-sputtered MEMS columns ($75\ \mu\text{m} \times 100\ \mu\text{m} \times 220\ \text{cm}$) coated with a $1.5\ \mu\text{m}$ -thick silica film. Solute: ethane, injected volume of $2\ \mu\text{L}$, and split ratio of 200. Carrier: He. Temperature: ambient temperature.

the kinetic behaviors of two columns. As illustrated by Fig. 6, the behavior of the two columns is very similar with the same optimum plate height (H) and velocity.

3.2. Semipacked columns

Applicability of silica sputtering to semipacked columns was also considered. The semipacked column consisted in a column including a network of square pillars ($10\ \mu\text{m} \times 10\ \mu\text{m}$).

The goal was to increase retention by increasing the surface area without modifying the thickness of the coating. Thus, the use of thick films, detrimental to efficiency, was avoided. For identical sputtering duration, SEM showed similar coatings thickness compared to open tubular columns (Fig. 3). A chromatogram obtained with this column is shown in Fig. 7. Compared with the open tubular column subjected to the same sputtering duration, the average retention increased 108%. Resolution between methane and ethane was also significantly improved; this improvement was not only a consequence of the higher retention; it also could be related to kinetic effects since efficiency increased. Fig. 8 provides a kinetic comparison of open tubular and semi-packed columns. Semi-packed columns provided around 5000 theoretical plates per

meter for propane, twice more than the equivalent open tubular column. As seen from these results, semi-packed columns are of interest not only because of the achievable gain in retention and capacity but also because they enable much higher efficiencies. However, further investigations, integrating extra column band broadening reduction, would be necessary to evaluate rigorously the C term part of the Van Deemter curve for semi-packed columns. Effectively, the experimental setup could not withstand pressures high enough to reach velocities exceeding $20\ \text{cm/s}$.

4. Conclusion

The present study and experiments demonstrated the potential of silica sputtering to coat GC MEMS columns using a process compatible with mass production and clean room facilities. Further characterization is required for the stationary phase obtained in this process, especially that of the physical coating: porosity and surface area. These parameters should be correlated to the chromatographic behavior of this “new” stationary phase. Nevertheless, the first chromatographic characterizations presented here are more than promising. Efficiencies observed, especially with semi-packed columns, are quite compatible with the requirements of a future autonomous GC MEMS sensor. With a view toward a wider scope of application, materials other than silica could also be considered (patent pending). The final aim of the project would be to propose a fully integrated MEMS system including injector [21,22] and detector [23] and optimized regarding extra column band broadening

References

- [1] K.D. Wise, *Sens. Actuators A: Phys.* 136 (2007) 39.
- [2] M.J.E. Golay, *Theory of Chromatography in Open and Coated Tubular Columns with Round and Rectangular Cross-Sections*, Gas Chromatography, Academic Press, New York, 1958, p. 36.
- [3] G.E. Spangler, *J. Microcolumn Sep.* 13 (2001) 285.
- [4] M. Agah, J.A. Potkay, G. Lambertus, R. Sacks, K.D. Wise, *J. Microelectromech. Syst.* 14 (2005) 1039.
- [5] S.C. Terry, J.H. Jerman, J.B. Angell, *IEEE Trans. Electron Devices* 26 (1979) 1880.
- [6] C.J. Lu, W.H. Steinecker, W.C. Tian, M.C. Oborny, J.M. Nichols, M. Agah, J.A. Potkay, H.K.L. Chan, J. Driscoll, R.D. Sacks, K.D. Wise, S.W. Pang, E.T. Zellers, *Lab Chip* 5 (2005) 1123.
- [7] B. Tienpont, F. David, P. Sandra, W. Witdouch, *LC-GC Europe* 22 (2009) <http://chromatographyonline.findanalytichem.com/lcgc/GC/Development-of-a-Miniature-Gas-Chromatograph-micro/ArticleStandard/Article/detail/585579>.
- [8] G. Lambertus, A. Elstro, K. Sensenig, J. Potkay, M. Agah, S. Scheuering, K. Wise, F. Dorman, R. Sacks, *Anal. Chem.* 76 (2004) 2629.
- [9] M. Stadermann, A.D. McBrady, B. Dick, V.R. Reid, A. Noy, R.E. Synovec, O. Bakajin, *Anal. Chem.* 78 (2006) 5639.
- [10] M.A. Zareian-Jahromi, M. Ashraf-Khorassani, L.T. Taylor, M. Agah, *J. Microelectromech. Syst.* 18 (2009) 28.
- [11] T. Nakai, S. Nishiyama, M. Shuzo, J.J. Delaunay, I. Yamada, *J. Micromech. Microeng.* 19 (2009) 1.
- [12] S.A. Greene, H. Pust, *Anal. Chem.* 29 (1957) 1055.
- [13] A.V. Kiselev, Y.U.S. Nikitin, R.S. Petrova, K.D. Shcherbakova, Y.A.I. Yashin, *Anal. Chem.* 36 (1964) 1526.
- [14] B. He, F. Regnier, *J. Pharm. Biomed. Anal.* 17 (1998) 925.
- [15] A. Fonverne, F. Ricoul, C. Demesmay, C. Delattre, A. Fournier, J. Dijon, F. Vinet, *Sens. Actuators B: Chem.* 129 (2008) 510.
- [16] S. Ali, M. Ashraf-Khorassani, L.T. Taylor, M. Agah, *Sens. Actuators B: Chem.* 141 (2009) 309.
- [17] L. Mondello, P. Quinto Tranchida, A. Casilli, O. Favoino, P. Dugo, G. Dugo, *J. Sep. Sci.* 27 (2004) 1149.
- [18] G.M. Gross, B.J. Prazen, J.W. Grate, R.E. Synovec, *Anal. Chem.* 76 (2004) 3517.
- [19] J. Tranchant, *Manuel pratique de chromatographie en phase gazeuse*, 4th edition, Masson, Paris, 1995, p. 441.
- [20] V.G. Berezkina, A.B. Lapin, J.B. Lipsky, *J. Chromatogr. A* 1084 (2005) 18.
- [21] K. Nachev, B. Bourlon, K. Danaie, P. Guieze, E. Donzier, F. Marty, *IEEE SENSORS 2009 Conference. The 8th Annual Conference on Sensors, 2009*, p. 1081, ISBN: 978-1-4244-4548-6, IEEE.
- [22] K. Nachev, T. Bourouina, F. Marty, B. Bourlon, K. Danaie, E. Donzier, *IEEE/ASME J. Microelectromech. Syst.* 19 (2010) 973.
- [23] Patent in press under the official international application number PCT/US10/52147.